tvst

Article

Abnormal Appearance of the Area Centralis in Labrador Retrievers With an *ABCA4* Loss-of-function Mutation

Björn Ekesten[1], Suvi Mäkeläinen[2,3], Stuart Ellis[4], Ulrika Kjellström[5], and Tomas F. Bergström[2]

[1] Department of Clinical Sciences, Swedish University of Agricultural Sciences, Uppsala, Sweden
[2] Department of Animal Breeding and Genetics, Swedish University of Agricultural Sciences, Uppsala, Sweden
[3] Department of Medical Biochemistry and Microbiology, Comparative Genetics and Functional Genomics, Uppsala University, Uppsala, Sweden
[4] The Veterinary Defence Society, Knutsford, UK
[5] Department of Clinical Science, Lund University, Lund, Sweden

Correspondence: Björn Ekesten, Department of Clinical Sciences, Swedish University of Agricultural Sciences, PO Box 7054, Uppsala SE-750 07, Sweden.
e-mail: bjorn.ekesten@slu.se

Received: May 27, 2021
Accepted: January 27, 2022
Published: February 24, 2022

Keywords: ABCA4; fovea; dog; animal model; Stargardt

Citation: Ekesten B, Mäkeläinen S, Ellis S, Kjellström U, Bergström TF. Abnormal appearance of the area centralis in labrador retrievers with an *ABCA4* loss-of-function mutation. Transl Vis Sci Technol. 2022;11(2):36, https://doi.org/10.1167/tvst.11.2.36

Purpose: To study retinal appearance and morphology in Labrador retrievers (LRs) heterozygous and homozygous for an *ABCA4* loss-of-function mutation.

Methods: Ophthalmic examination, including ophthalmoscopy and simple testing of vision, was performed in five $ABCA4^{wt/wt}$, four $ABCA4^{wt/InsC}$, and six $ABCA4^{InsC/InsC}$ LRs. Retinas were also examined with confocal scanning laser ophthalmoscopy (cSLO) and optical coherence tomography (OCT). Infrared and fundus autofluorescence (FAF) images were studied, and outer nuclear layer (ONL) and neuroretinal thickness were measured in the central and peripheral area centralis.

Results: Clinical signs in young $ABCA4^{InsC/InsC}$ LRs were subtle, whereas ophthalmoscopic findings and signs of visual impairment were obvious in old $ABCA4^{InsC/InsC}$ LRs. Retinal appearance and vision testing was unremarkable in heterozygous LRs regardless of age. The cSLO/OCT showed abnormal morphology including ONL thinning, abnormal outer retinal layer segmentation, and focal loss of retinal pigment epithelium in the fovea equivalent in juvenile $ABCA4^{InsC/InsC}$ LRs. The abnormal appearance extended into the area centralis and visual streak in middle-aged $ABCA4^{InsC/InsC}$ and then spread more peripherally. A mild phenotype was seen on cSLO/OCT and FAF in middle-aged to old $ABCA4^{wt/InsC}$ LRs.

Conclusions: Abnormal appearance and morphology in the fovea equivalent are present in juvenile $ABCA4^{InsC/InsC}$. In the older affected LRs, the visual streak and then the peripheral retina also develop an abnormal appearance. Vision deteriorates slowly, but some vision is retained throughout life. Older heterozygotes may show a mild retinal phenotype but no obvious visual impairment. The $ABCA4^{InsC/InsC}$ LR is a potential model for *ABCA4*-mediated retinopathies/juvenile-onset Stargardt disease in a species with human-sized eyes.

Translational Relevance: The $ABCA4^{InsC}$ mutation causes juvenile-onset abnormal appearance of the fovea equivalent in affected dogs that slowly spreads in the retina, while only a mild phenotype is seen in older carriers. This is the first non-primate, large-animal model for ABCA4-related/STGD1 retinopathies in a species with a fovea equivalent.

Introduction

The retinal-specific ATP-binding cassette transporter (ABCA4) is a protein facilitating the removal of excessive 11-*cis*-retinal and toxic retinoid compounds from the disks of the photoreceptor outer segments.[1,2] The protein is also present at low concentrations in the retinal pigment epithelium (RPE), probably to enhance endolysosomal function and thereby prevent

accumulation of lipofuscin.[3] Abnormal function of the ABCA4 protein, caused by any of the more than 1000 known mutations in the *ABCA4* gene, is known to cause a spectrum of retinal diseases ranging from Stargardt macular dystrophy to progressive cone dystrophy (CD) or cone-rod dystrophy (CRD).[4,5] Autosomal recessive Stargardt disease (STGD1) (OMIM: 248200) is most often a juvenile macular dystrophy. Empirically, the prevalence has been estimated at one in 8000 to 10,000,[6] and in a recent study based on available whole-genome and whole-exome sequence, the genetic prevalence for STGD1 was estimated to 1:6578.[7] Central vision typically deteriorates rapidly during the first two decades of life, but a milder, late-onset form with foveal sparing has also been described.[8] The phenotypic variation has been attributed to the severity of the *ABCA4* mutation with loss-of-function mutations causing earlier onset and more rapid progression than less deleterious variants with residual ABCA4 function, but genetic modifiers and environmental factors may also be of importance for the course of the disease.[9–11]

Interestingly, human carriers for *ABCA4* mutations may also present with abnormal macular function as determined by multifocal electroretinography (ERG) and, less frequently, also abnormal full-field, cone-driven ERGs, although visual complaints seem very rare.[12,13] Furthermore, mild pigmentary changes in the macular area, altered fundus autofluorescence (FAF), and outer retinal disruption on optical coherence tomography (OCT) b-scans can be found in some heterozygous individuals, but certainly not all.[12,14] As in STGD1 patients, the heterogeneity in clinical phenotypes in heterozygotes is suggested to reflect the severity of the *ABCA4* mutation. Hence, the mode of inheritance could be considered as incomplete dominant for some forms of STGD, rather than recessive.

Currently, there is no therapy for STGD1, but patients are recommended to avoid excessive intake of vitamin A and exposure to ultraviolet light. The impact on the daily lives of human patients of this disease, characterized by rather high prevalence, mostly early onset, and usually severe impairment in central vision, has led to a search for suitable treatments, both for patients with early signs of STGD1 and mild retinal changes, as well as patients with advanced disease and substantial loss of normal retinal architecture. Several clinical trials with drugs directly or indirectly targeting the visual cycle, as well as gene and stem cell therapies, have been attempted or are ongoing in human patients (see Rahman et al. 2020[6] for review).

We have recently identified a mutation in the *ABCA4* gene (CanFam3.1 Chr6:55,146,550–55,146,556, c.4176insC) in the Labrador retriever (LR)[15] causing a loss-of-function of the ABCA4 protein (p.F1393Lfs*1395) leading to abnormal retinal appearance and function in affected dogs. In contrast to human Stargardt patients, who often are compound heterozygotes with two different *ABCA4* mutations, the affected LRs examined were all homozygous for the same loss-of-function mutation.

This is the first non-primate, large-animal model with a naturally occurring mutation in the *ABCA4* gene. Although dogs are dichromats with lower cone densities and less well-developed fovea-like, cone-rich areas for central vision than human beings,[16,17] we believe that characterization of this disease in the LR can provide comparative insights into *ABCA4*-mediated retinopathies/juvenile-onset STGD1. Furthermore, the shared phenotypic similarities and the approximately human-sized eye in this species with a fovea-like area for central vision opens up for future studies of therapeutic interventions, including gene therapy.

Material and Methods

In total, 16 privately owned Labrador retrievers were examined (Table 1). Five dogs were homozygous for the wildtype allele ($ABCA4^{wt/wt}$), five were heterozygous (carriers) for the mutation ($ABCA4^{wt/InsC}$), and six dogs were homozygous for the mutation ($ABCA4^{InsC/InsC}$). Some of the affected dogs and carriers were closely related (Fig. 1).

Ophthalmic examinations were performed, and blood samples for DNA testing were obtained with informed dog owner consent. Some dogs were only available for routine ophthalmic examination and not for or only partially for the cSLO/OCT examinations. All examinations and handling of animals adhered to the ARVO Animal Statement. Ethical approval was granted by the regional animal ethics committee (Uppsala djursförsöksetiska nämd; Dnr C12/15, Dnr 5.8.18-15533/2018, Dnr 5.8.18-04682/2020 and C148/13).

Whole blood samples were collected in EDTA tubes and genomic DNA was extracted using 1 mL blood on a QIAsymphony SP instrument and the QIAsymphony DSP DNA Kit (Qiagen, Hilden, Germany). Previously designed sequencing primers[15] with M13 sequencing tails (Cfa_ABCA4_Frw: 5′-tgtaaaacgacggccagtCACCCACATTGCCATGTTTA-3′, Cfa_ABCA4_Rev: caggaaacagctatgaccAACACA-TGGGGGTGAATGAT-3′ were used to amplify a 201 bp region extending from intron 27–28 to intron 28–29 of the canine *ABCA4* gene. The amplicons

Table 1. Demographics of the LR Dogs Studied

Dog	ABCA4 Genotype	Gender	Age at Exam [mo]	Exams	Age at Re-Exam [mo]	Exams	Age at Re-Exam [mo]	Exams
AF1	InsC/InsC	M	9	Oph	11	Oph, cSLO	25	Oph, cSLO, OCT
AF2	InsC/InsC	F	25	Oph, cSLO, OCT	—	—	—	—
AF3	InsC/InsC	F	61	Oph, cSLO	75	Oph, cSLO, OCT	—	—
AF4	InsC/InsC	M	93	Oph	—	—	—	—
AF5	InsC/InsC	F	128	Oph, cSLO, OCT	—	—	—	—
AF6	InsC/InsC	M	140	Oph, cSLO	—	—	—	—
CA1	wt/InsC	M	11	Oph, cSLO	—	—	—	—
CA2	wt/InsC	F	22	Oph, cSLO, OCT	—	—	—	—
CA3	wt/InsC	F	61	Oph, cSLO, OCT	—	—	—	—
CA4	wt/InsC	F	93	Oph, cSLO, OCT	—	—	—	—
CA5	wt/InsC	M	149	Oph, cSLO, OCT	—	—	—	—
WT1	wt/wt	M	15	Oph, cSLO, OCT	—	—	—	—
WT2	wt/wt	F	26	Oph, cSLO, OCT	—	—	—	—
WT3	wt/wt	F	47	Oph, cSLO, OCT	—	—	—	—
WT4	wt/wt	M	124	Oph, cSLO, OCT	—	—	—	—
WT5	wt/wt	F	141	Oph, cSLO, OCT	—	—	—	—

Wt, wildtype allele; insC, mutant allele; F, female; M, male; mo, months; Oph, ophthalmic examination including indirect ophthalmoscopy.

were sequenced using BigDye Direct Cycle Sequencing Kit (Applied Biosystems, Thermo Fisher Scientific, Waltham, MA) on an Applied Biosystems 3500 Series Genetic Analyzer. In addition, all samples were genotyped using a real-time polymerase chain reaction assay. A genotyping assay was designed using the Custom TaqMan Assay Design Tool (Thermo Fisher Scientific) The assay mix

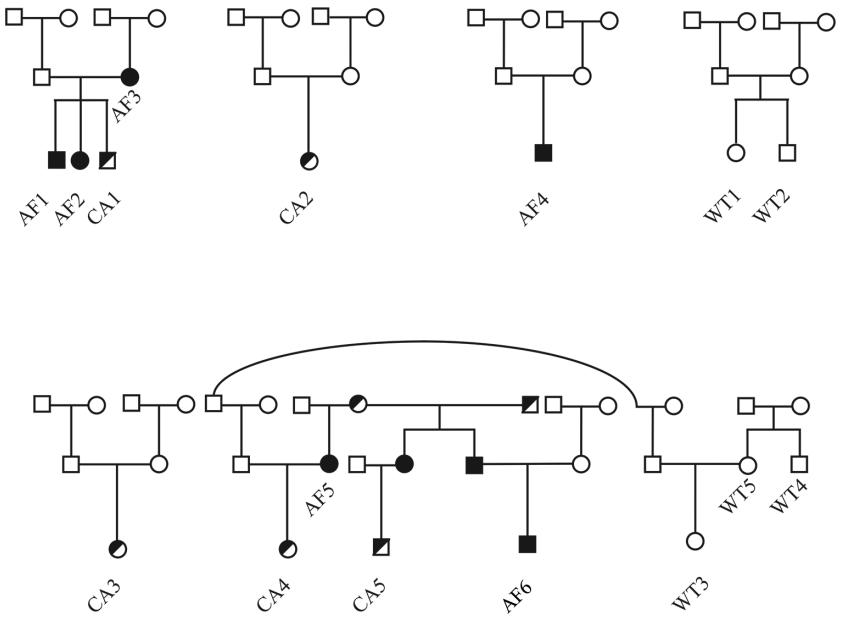

Figure 1. Pedigree showing the kinship between the dogs included in the study. *Open symbols* represent individuals that do not have known history of visual impairment. Individuals genotyped wild-type (ABCA4$^{wt/wt}$) are indicated with WT. *Half-closed symbols* represent individuals that are genotyped heterozygous for the insertion (ABCA4$^{wt/InsC}$), and *closed symbols* represent individuals that are genotyped homozygous for the insertion (ABCA4$^{InsC/InsC}$). All dogs except AF4, as well as WT1 and WT2, have common ancestors in the fifth or sixth generation (data not shown).

included the amplification primers Labbe_F (5′-GTTTTTGGCTCTGATGCTTTCCAT-3′) and Labbe_R (-5′-GGGTGAAGGATCAAAGCAGGATATT-3′) and probes specific for the insertion (VIC-5′-TTGTCCCCCCCCTTTG-3′) and for the wildtype (FAM-5′-ATTGTCCCCCCCTTTG-3′). Genomic DNA (50–100 ng), ProAmp mastermix (Applied Biosystems) and water was added to a final volume of 10 µL and the amplification and detection was performed on a StepOnePlus Real-Time polymerase chain reaction system (Applied Biosystems) with standard cycling conditions for a custom TaqMan SNP assay (an initial hold at 95°C for 10 minutes followed by a total of 40 cycles at 95°C for 15 seconds and 60°C for 40 seconds).

Ophthalmic examination included reflex testing, testing of vision with falling cotton balls under dim light and daylight conditions, as well as indirect ophthalmoscopy (Heine 500; Heine Optotechnik GmbH, Herrsching, Germany) and slit-lamp biomicroscopy (Kowa SL-17; Kowa Company Ltd., Tokyo, Japan) after dilation of pupils with tropicamide (Tropikamid Bausch Lomb 0.5%; Bausch & Lomb Nordic AB, Stockholm, Sweden).

Retinas were also examined using cSLO and scanned with OCT horizontally along the visual streak (Spectralis HRT + OCT; Heidelberg Engineering GmbH, Heidelberg, Germany) after light sedation with medetomidine 0.01 mg/kg intramuscularly (Sedator vet.; Dechra Veterinary Products AB, Upplands-Väsby, Sweden) (Table 1). The corneas were kept moist using artificial tears (Aptus SentrX; Orion Pharma Animal Health, Danderyd, Sweden). Infrared confocal ophthalmoscopy (IR) and FAF were performed using IR (820 nm) and blue lasers (488 nm), respectively, using non-normalized sampling mode. Neuroretinal thickness and ONL thickness were measured at the fovea-like center of the area centralis and 0.5 mm nasally and temporally to the fovea equivalent along a horizontal line in 5 $ABCA4^{wt/wt}$, 4 $ABCA4^{wt/InsC}$ and 4 $ABCA4^{InsC/InsC}$ eyes from age-matched LRs.

Screening for differences in ONL thickness between genotypes was performed using standard statistical software (the Kruskal-Wallis test in JMP Pro 15.2.1; SAS Institute Inc., Cary, NC, USA). Dunn's test with wildtype LRs as control group was used as post hoc test. A P value <0.05 was considered statistically significant.

Results

Clinical signs in young LRs homozygous for the mutation (≤25 months of age) were subtle and could easily be missed on routine ophthalmic examination. Reflex testing was normal. Testing vision with falling cotton balls in normal room light and under dim light conditions was either completely normal under both lighting conditions or ambiguous in room light, but improved when the light was dimmed. Ophthalmoscopically, an affected male appeared normal at the age of nine months. At the age of almost one year and later, at two years of age, a less than a millimeter–sized area of dull tapetal reflection, like a pin-prick, was observed approximately 5 mm dorsotemporal to the optic nerve head coinciding with the central part of the area centralis in both eyes (Fig. 2). Similar ophthalmoscopic findings were seen in his two-year-old sister ($ABCA4^{InsC/InsC}$). Very mild vascular attenuation was also observed in the area centralis in these dogs at the age of two years. Findings were bilateral and similar between the eyes.

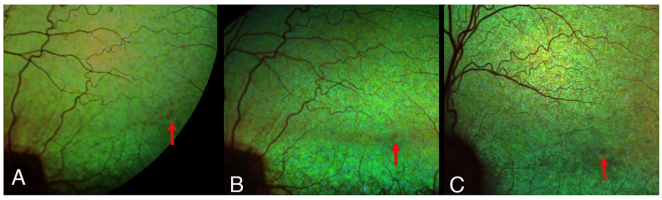

Figure 2. The fundus of the left eye of (A) an 11-month-old $ABCA4^{InsC/InsC}$ Labrador retriever (AF1). (B) The same dog at 25 months of age, and (C) an affected $ABCA4^{InsC/InsC}$ dog at the age of 61 months (AF3). *Red arrows* show the hyporeflective, grayish fovea equivalent. In (B), the altered tapetal reflectivity has spread along the horizontal, cone-rich visual streak. In the older affected dog (C), the dull tapetal reflection is also seen outside the visual streak and attenuation of the retinal vessels is more evident.

In middle-aged affected LRs (61–93 months old), reflexes were typically normal, as well as vision testing with cotton balls under dim light conditions. Both dogs also readily detected falling cotton balls in room light, but in one of five trials the response was judged ambiguous. The tapetal reflection was altered in a larger portion of the area centralis and visual streak. Typically, a darker (hyporeflective), dull mottling effect was best seen when the indirect ophthalmoscopy lens was tilted slightly back and forth. As a consequence of the more abnormal tapetal reflection in the middle-aged dogs, the pin-prick-like lesion in the area centralis became less well outlined. Mild attenuation of retinal blood vessels was also seen. Tapetal hyper-reflection was not a typical finding even in old LRs, but a match-like, horizontal, hyper-reflective band corresponding to the visual streak with the area centralis (as the head of a match) was observed in both eyes of an almost eight-year-old dog (AF3).

Mildly or moderately dilated pupils and sluggish PLRs were seen in old LRs homozygous for the mutation (≥128 months old), whereas dazzle reflexes and menace responses were often, but not always

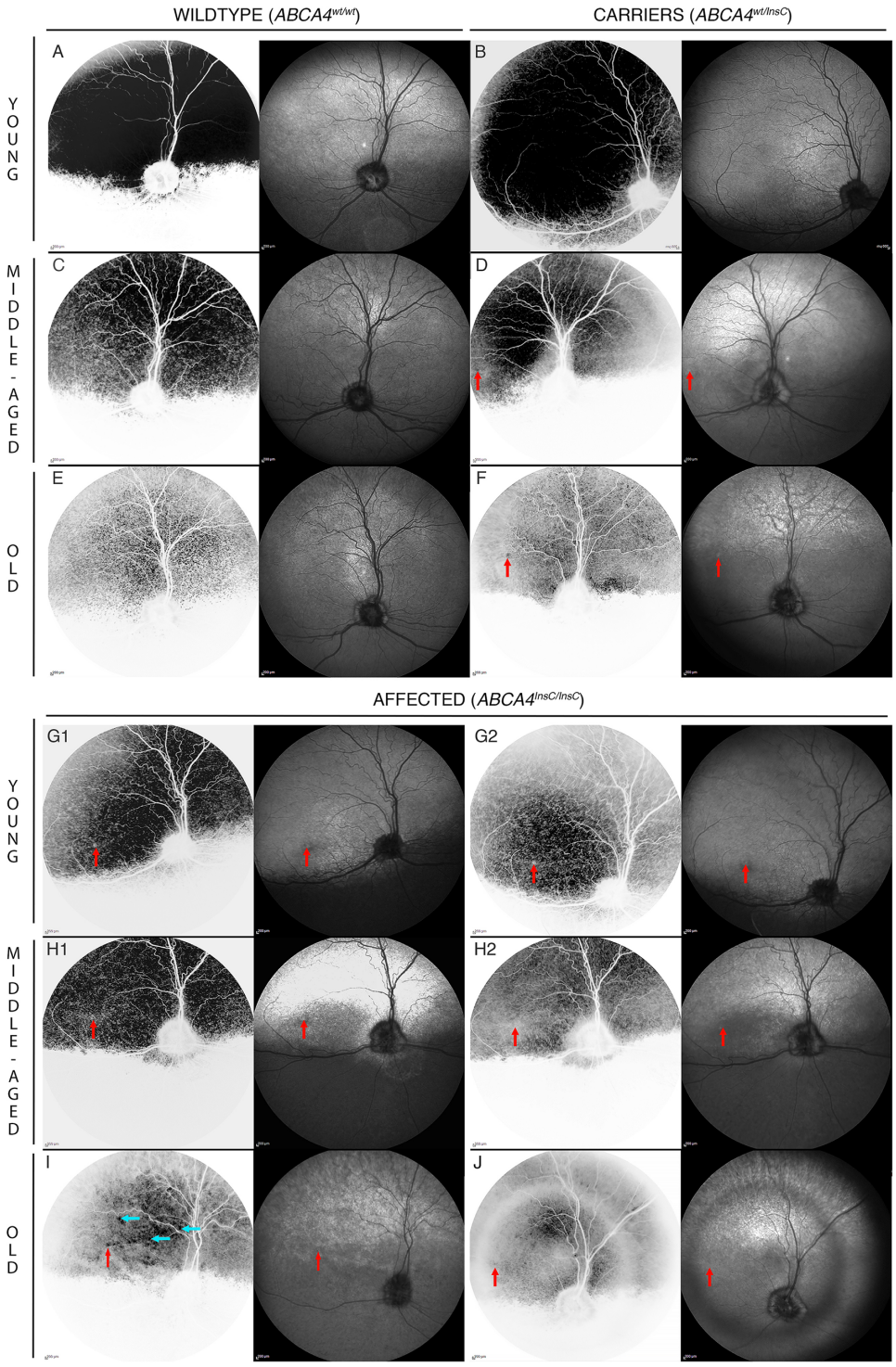

Figure 3. Inverted FAF (*white background*) and IR images (*black background*) of the right fundus of 10 Labrador retrievers subdivided in young (11–26 months old), middle age (47–93 months) and old (141–149 months). (A), (C) and (E) show WT2, WT3 and WT 4, (B), (D) and (F) are photos from CA1, CA4 and CA5. (G1) and (G2) show increasing areas of decreased FAF in area centralis and visual streak interpreted as progressive decrease in RPE density from the age of 11 months and 25 months in AF1. (H1) and (H2) display the decrease in FAF both in and outside the visual streak and progressive vascular attenuation in AF3 at 61 and 75 months of age, respectively. (I) *Blue arrows* show small areas of bright autofluorescence in the tapetal area in AF5. (J) In AF6, magnification of the central part of the fundus and the halo-like phenomenon is caused by lenticular, nuclear sclerosis. *Red arrows* indicate the position of the fovea-like center of the area centralis, which is discernible in older heterozygotes and all affected dogs.

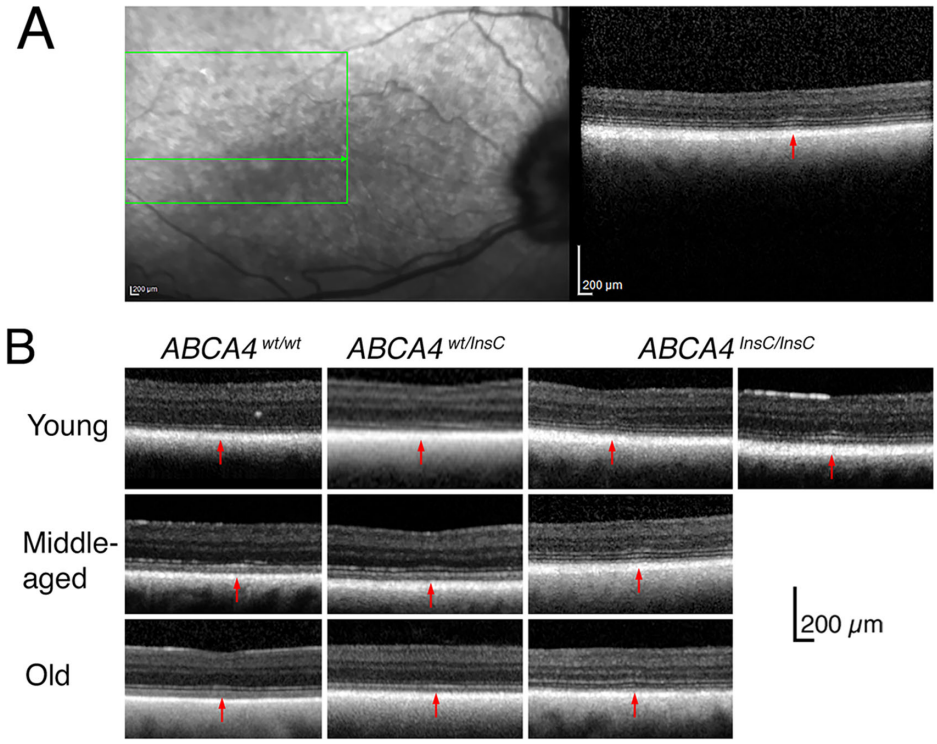

Figure 4. (A) IR cSLO-image of the right fundus of a 75-month-old affected dog *ABCA4*$^{InsC/InsC}$ (AF3). The fovea-like area is brighter than the surrounding hyporeflective part of the visual streak. The OCT-scan is taken through the fovea-like area (*red arrow*) where a thin ONL, a thickened, hyperreflective, and slightly irregular ELM and slightly hyperreflective and thickened EZ are seen. (B) OCTs through the fovea-like area showing chiefly reduced outer retinal thickness in affected LRs, more obvious in older dogs than younger (young, 15–25 months; middle-aged, 47–61 months; old, 128–149 months). The morphology of the fovea-like area of wildtype LRs and heterozygotes appear very similar. *Red arrows:* fovea-like area.

consistently maintained in one of these two dogs. Vision testing with falling cotton balls indicated both impaired daylight and dim light vision. Photophobia was noticed in an almost 12-year-old male (AF6), but not in any of the other affected dogs. Retinal vascular attenuation was evident but not particularly striking given the senescence of these dogs. All of, or at least a substantial part of, the tapetal fundus showed abnormal light reflection when the ophthalmoscopy lens was tilted back and forth.

Reflex and falling cotton ball testing in carriers (*ABCA4*$^{wt/InsC}$) were normal and ophthalmoscopy showed normal appearance of the ocular fundus regardless of the age of the dog. Hence, the carriers could neither be distinguished from LRs homozygous for the wild-type allele (*ABCA4*$^{wt/wt}$) on reflex and response testing, nor on indirect ophthalmoscopy.

IR cSLO showed focal hyporeflection surrounding the normoreflective or partially hyporeflective center of the area centralis in the youngest affected dogs. The hyporeflective area extended into the surrounding area centralis and along the visual streak in middle-aged dogs, whereas the central fovea-like area appeared bright (Fig. 3). Eventually, the entire tapetal fundus appeared mottled in old affected LRs. The fundus of young carriers appeared normal on IR cSLO. In older carriers, the brighter fovea-like center of the area centralis was surrounded by a ring that appeared hyporeflective, which was most evident in the oldest dog.

The tapetal reflection of blue light cSLO decreased with age in all LRs regardless of genotype. Decreased FAF was most evident in the fovea-like area of young affected LRs but spread along the visual streak in older dogs (Fig. 3), indicating a progressive reduction of the RPE in the most cone-rich areas. In old affected LRs, islets of increased FAF were observed in the tapetal area, whereas a more uniform autofluorescence was seen in the nontapetal area. Interestingly, middle age and old carriers showed increased FAF confined to the fovea-like area indicating localized accumulation of lipofuscin, whereas a very mild decrease in FAF was seen along the visual streak.

OCTs through the fovea-like area showed either an almost flat vitreo-retinal border (fovea plana) or a subtly indented inner retinal surface (corresponding to

Table 2. ONL and Neuroretinal Thickness (Mean ± SD)*

	ONL			Neuroretina		
	Nasal	Center	Temporal	Nasal	Center	Temporal
ABCA4$^{wt/wt}$ [µm]	46 ± 7	44 ± 5	45 ± 4	191 ± 12	182 ± 11	189 ± 13
ABCA4$^{wt/InsC}$ [µm]	33 ± 4	28 ± 9	32 ± 4	178 ± 8	165 ± 12	176 ± 10
ABCA4 $^{InsC/InsC}$ [µm]	28 ± 7	16 ± 7	27 ± 8	169 ± 12	164 ± 11	169 ± 15
ABCA4$^{wt/wt}$ *vs ABCA4*$^{wt/InsC}$	$P = 0.13$	$P = 0.17$	$P = 0.09$	$P = 0.31$	n/a	n/a
ABCA4$^{wt/wt}$ *vs ABCA4* $^{InsC/InsC}$	$P = 0.02$	$P = 0.004$	$P = 0.01$	$P = 0.034$	n/a	n/a

SD, standard deviation; n/a, post hoc testing was not applicable, because no statistically significant difference was found when data from all three genotypes were compared.

*From OCTs in the center and 0.5 mm nasally and temporally of the fovea-like area and post hoc statistics with *ABCA4*$^{wt/wt}$ as control group.

a shallow "foveal pit"; Fig. 4). This minute difference in retinal morphology neither seemed to be related to age nor genotype of the dog. In the 2-year-old affected LRs, outer retinal thinning (including thinning of the outer nuclear layer, ONL) was evident in the fovea-like area and surrounding area centralis compared to age-matched normal dogs (Fig. 4). Thinning of the outer retina and ONL in the fovea-like area and positions 0.5 mm temporal and nasal to it was even more evident in older affected dogs where the ONL was <50% of that in normal LRs. In carriers, ONL thickness in these regions took an intermediate position between normal and affected dogs. The ONL of affected LRs was significantly thinner in the fovea-like area ($p = 0.004$), as well as nasally and temporally to the fovea-like area than in wildtype LRs ($p = 0.02$ and $p = 0.01$, respectively), whereas the difference between wildtype and heterozygous LRs was not statistically significant (Table 2). Either or both of the external limiting membrane (ELM) and ellipsoid zone (EZ) appeared thickened and hyperreflective in the fovea equivalent in the *ABCA4*$^{InsC/InsC}$ LRs.

Discussion

The loss-of-function mutation in *ABCA4* recently described in LR dogs[15] can cause clinical signs in the retina of affected dogs by1 year of age. The ophthalmoscopic signs are subtle and IR and FAF imaging facilitates detection of the abnormal appearance of the fovea-like area and surrounding area centralis. Although there are more or less scientific ways to convert the age of a dog to human years,[18,19] the onset is no doubt juvenile. The age of the youngest dog with evident ophthalmoscopic and cSLO findings in the fovea equivalent would approximately translate to a human subject in their teens or twenties depending on the age conversion formula preferred.

The localization and the focal FAF hypofluorescence in the fovea-like center of the area centralis mimic forms of childhood-onset STGD and correspond to the mildly abnormal foveal appearance and FAF patterns sometimes seen in young human patients.[10] Although a decrease in FAF may be caused both by loss of RPE and photobleaching of bisretinoid fluorophores in aging human patients,[20] we believe that the decrease in FAF in the fovea-like center and its surround in affected LRs is more likely to reflect loss of RPE rather than photobleaching of aged lipofuscin, as this was observed already in young dogs.

The canine fovea equivalent, surrounding area centralis and its horizontal extension, the visual streak, are all located in the tapetal fundus of the dog, where the RPE overlying the tapetum lucidum is non-pigmented.[16,21] Both the tapetal reflectivity and tapetal color change in puppies, but the tapetal reflection is considered to be adult-like within the first three months of life.[22] Hence, abnormal tapetal reflection in affected young dogs cannot be attributed to their youth. The marked decrease in overall tapetal reflection with age seen with short-wavelength cSLO (FAF-settings) but not evident on IR-images, has not been described previously to the best of our knowledge. We have not explored the reason for this decrease further, but it was observed regardless of genotype. It has been suggested that the number of tapetal cell layers decrease with age in the dog and thereby, both the tapetal reflectivity as well as the tapetal area decrease.[23] Reduced transmission of short-wavelength light through the aging optic media, neuroretina and RPE may also contribute to the fainter tapetal reflection.

RPE atrophy has been suggested both to precede and be secondary to photoreceptor degeneration in STGD1 patients.[24,25] Either way, the RPE may

be overloaded with shedded outer segment material containing toxic bisretinoids when ABCA4 is dysfunctional in the photoreceptors. Additionally, functional ABCA4 in the RPE has also been shown to be important for maintaining both the RPE and photoreceptors.[3] In middle-aged affected LRs, the FAF-hyporeflection suggestive of RPE atrophy extended well outside the fovea-like area and into the area centralis and visual streak. In the oldest STGD dogs, the RPE atrophy had spread to the peripheral retina. This is in agreement with several reports on progressive RPE atrophy in both human patients and transgenic mice with mutations in the *ABCA4* gene.[26–28] RPE atrophy was not a typical finding on histopathology in our previous article,[15] but samples were taken more peripherally and nasally (opposite side to the fovea equivalent) and the results may therefore reflect either individual or regional differences or both. In old dogs, bleaching of the retinal fluorophores over the years may contribute to a reduction in FAF, as reported in human patients with some forms of recessive Stargardt disease.[20] We observed diffuse, increased FAF in the nontapetal area in old affected LRs. Lipofuscin has been described as the dominant fluorophore in the retina and was observed in the RPE of affected dogs in our previous study,[15] but other retinal fluorophores such as photooxidized bisretinoids also autofluoresce.[29] Thus accumulation of phototoxic bisretinoids (including A2E) is likely to contribute to the increase in FAF seen in *ABCA4*$^{InsC/InsC}$ *LRs*.

The cSLO IR-hyporeflection, as well as the abnormal tapetal reflection and retinal vascular attenuation also seen on ophthalmoscopy was more evident in older affected dogs and not restricted to the area centralis surrounding the fovea equivalent indicating a diffuse, widespread retinal degeneration in old LRs. This is in agreement with electroretinographic, histopathologic and immunofluorescent findings in the old affected LRs previously reported.[15] Thus this loss-of-function mutation causes neuroretinal and RPE degeneration slowly spreading from the fovea-like area, into the midperiphery and further toward the peripheral fundus, mimicking the progression from Stargardt macular dystrophy to cone-rod dystrophy seen in some human patients with *ABCA4* mutations.[10,11,26,30–32] A more widespread retinal degeneration causing a reduction of both cones and rods was further supported by OCTs showing retinal thinning, most evident in middle-aged and older affected LRs, with normal appearing inner retina and thinning of the ONL. The thinning of the ONL in the fovea-like area and 0.5 mm nasally and temporally to this position was even statistically significant despite the low number of dogs included in this study. Because rods outnumber cones by far in both the area centralis and peripheral retina,[17] the ONL thinning indicates that not only cones have been lost, but also rods. The abnormal appearance of outer retinal structure in the fovea equivalent of young affected LRs mimic findings in childhood-onset STGD1.[10]

Yellowish flecks are a hallmark in human STGD1 but may not be present in children with early-onset forms of the disease.[10] Furthermore, flecks are not typically seen in CRD associated with *ABCA4* mutations.[33–35] We were not able to convincingly detect flecks in or near the fovea-like area, either by ophthalmoscopy or cSLO. One reason may be that flecks are not a typical finding in LRs with this mutation; another potential reason is the inherent difficulty to detect such yellowish material in dogs where the tapetum lucidum often has a bright yellow to greenish reflection. None of the dogs reported in this current study developed the widespread mottled brownish deposits in the tapetal area that were present in one of the dogs in our previous report.[15]

Interestingly, the middle-aged and older carriers for the mutation studied showed a mild phenotype characterized by accumulation of lipofuscin in the RPE in the fovea-like area. Although simple vision testing and ophthalmoscopy were considered unremarkable in these dogs regardless of age, both IR- and FAF-cSLO showed abnormal appearance in the fovea-like area (and very subtly in the visual streak). On OCTs, the ONL thickness in carriers fell in between that of age-matched, wildtype and affected LRs, although the difference was not statistically significant. The majority of human carriers for *ABCA4* mutations are not considered to show a clinically abnormal phenotype,[14] although heterozygotes for some mutations may have both abnormal retinal function and morphology causing visual impairment detectable in at least some patients on psychophysical testing.[12,13] Although very rare, a mild retinal phenotype has been reported in human heterozygotes for *ABCA4* mutations. A male with 20/20 visual acuity being heterozygous for the splice site variant c.5714+5G>A was reported to have parafoveal pisciform flecks corresponding to disruption of the EZ- and RPE-bands on OCT.[36] Furthermore, a fine granular FAF-pattern with peripheral punctate spots, a phenotype associated with human age-related macular degeneration patients, was recently attributed to monoallelic *ABCA4* mutations rather than risk increasing AMD alleles[37] again indicating that some ABCA4 mutations may cause a phenotype in carriers. The loss-of-function mutation in the LRs causes a premature translation stop codon, and our previous results indicate that the truncated mRNA-fragments

are likely to be targeted by nonsense-mediated decay.[15] Such a serious mutation would therefore result in a loss of the ABCA4 protein, which is likely to be the reason for the abnormal morphology observed in elderly canine carriers.

The impact of the *ABCA4* loss-of-function mutation in Labrador retrievers, most of them field-trial type dogs, was variable, as reported by their owners and trainers. The performance of young, affected LRs ranged from normal to having unexpected problems detecting markings (falling birds or dummies) at a distance. Our attempts to crudely assess vision suggested that daylight vision was impaired in at least some dogs early in life, whereas concomitant impaired dim-light vision was seen mainly in old dogs. However, these old dogs, close to the end of a normal LR lifetime, still retained some vision allowing them to live a relatively normal life as companion animals, as reported by the owners. We were neither able to detect signs of visual impairment in heterozygotes for this mutation (some of them field-trial champions), nor did we receive anecdotal evidence from their owners suggesting that the performance of these dogs was affected even at old age. The lack of signs of impaired vision may also reflect that the methods used for testing vision were far too insensitive and that these dogs may rely less on high-acuity vision for solving tasks included in the daily life of a retriever. Furthermore, human carriers for *ABCA4* mutations have been reported to have normal visual acuity, although multifocal ERG revealed abnormal macular function.[12]

We have previously reported on retinal function assessed with ERG in two LRs homozygous for and one LR heterozygous for the *ABCA4* loss-of-function mutation.[15] Further assessment of retinal function in both affected dogs and carriers would, of course, be valuable. However, we have been studying this mutation in privately-owned dogs, which limited both number and type of procedures the owners consent to. A colony of dogs with this *ABCA4* mutation will provide better opportunity to study this disease in greater detail.

In summary, the spontaneous, loss-of-function *ABCA4* mutation results in abnormal appearance and morphology of the fovea-like center of the area centralis, including outer retinal thinning compared to age-matched wildtype LRs, abnormal segmentation of the outer retinal layers seen on OCT and focal loss of RPE, already in juvenile LRs. In older dogs, the abnormal appearance has spread into the area centralis and visual streak and later on, into the more peripheral fundus indicating a progression from a canine equivalent to a foveopathy to a diffuse cone-rod degeneration. Vision slowly deteriorates, but some vision seems to be retained throughout a normal LR lifetime. Older heterozygotes may show a mild phenotype with increased FAF in the fovea-like area, but visual impairment could neither be detected using simple testing nor was revealed in the history of such a dog.

Knock-out mouse models provided important information about *ABCA4* retinopathies but are not precise models of human disease.[38] Furthermore, the small size of the globe, the lack of a fovea or fovea-like area and difficulty to train mice for more advanced behavioral testing limit the usefulness of murine models. Because of similarities in retinal morphology between affected LRs and more severe forms of juvenile-onset STGD1 in human patients, as well as the human-like size of the globe in this species with a fovea-like area, we believe the affected LR is a suitable large-animal model for both basic science research and development of novel therapeutic interventions.

Acknowledgments

Supported by the Swedish Research Council FORMAS and the AGRIA and Swedish Kennel Club research foundation.

Disclosure: **B. Ekesten,** None; **S. Mäkeläinen,** None; **S. Ellis,** None; **U. Kjellström,** None; **T.F. Bergström,** None

References

1. Quazi F, Lenevich S, Molday RS. ABCA4 is an N-retinylidene-phosphatidylethanolamine and phosphatidylethanolamine importer. *Nat Commun.* 2012;3:1–9.
2. Quazi F, Molday RS. ATP-binding cassette transporter ABCA4 and chemical isomerization protect photoreceptor cells from the toxic accumulation of excess 11-cis-retinal. *Proc Natl Acad Sci USA*. 2014;111:5024–5029.
3. Lenis TL, Hu J, Ng SY, et al. Expression of ABCA4 in the retinal pigment epithelium and its implications for Stargardt macular degeneration. *Proc Natl Acad Sci USA*. 2018;115:E11120–E11127.
4. Gill JS, Georgiou M, Kalitzeos A, Moore AT, Michaelides M. Progressive cone and cone-rod dystrophies: clinical features, molecular genetics and prospects for therapy. *Br J Ophthalmol*. 2019;103:711–720.
5. Tanna P, Strauss RW, Fujinami K, Michaelides M. Stargardt disease: clinical features, molecular

genetics, animal models and therapeutic options. *Br J Ophthalmol*. 2017;101:25–30.
6. Rahman N, Georgiou M, Khan KN, Michaelides M. Macular dystrophies: clinical and imaging features, molecular genetics and therapeutic options. *Br J Ophthalmol*. 2020;104:451–460.
7. Hanany M, Rivolta C, Sharon D. Worldwide carrier frequency and genetic prevalence of autosomal recessive inherited retinal diseases. *Proc Natl Acad Sci USA*. 2020;117:2710–2716.
8. Westeneng-van Haaften SC, Boon CJ, Cremers FP, Hoefsloot LH, den Hollander AI, Hoyng CB. Clinical and genetic characteristics of late-onset Stargardt's disease. *Ophthalmology*. 2012;119:1199–1210.
9. Fujinami K, Sergouniotis PI, Davidson AE, et al. Clinical and molecular analysis of Stargardt disease with preserved foveal structure and function. *Am J Ophthalmol*. 2013;156:487–501.e481.
10. Fujinami K, Zernant J, Chana RK, et al. Clinical and molecular characteristics of childhood-onset Stargardt disease. *Ophthalmology*. 2015;122:326–334.
11. Kjellstrom U. Association between genotype and phenotype in families with mutations in the ABCA4 gene. *Mol Vis*. 2014;20:89–104.
12. Kjellstrom U. Reduced macular function in ABCA4 carriers. *Mol Vis*. 2015;21:767–782.
13. Maia-Lopes S, Silva ED, Silva MF, Reis A, Faria P, Castelo-Branco M. Evidence of widespread retinal dysfunction in patients with Stargardt disease and morphologically unaffected carrier relatives. *Invest Ophthalmol Vis Sci*. 2008;49:1191–1199.
14. Duncker T, Stein GE, Lee W, et al. Quantitative fundus autofluorescence and optical coherence tomography in ABCA4 carriers. *Invest Ophthalmol Vis Sci*. 2015;56:7274–7285.
15. Mäkeläinen S, Godia M, Hellsand M, et al. An ABCA4 loss-of-function mutation causes a canine form of Stargardt disease. *PLoS Genet*. 2019;15:e1007873.
16. Beltran WA, Cideciyan AV, Guziewicz KE, et al. Canine retina has a primate fovea-like bouquet of cone photoreceptors which is affected by inherited macular degenerations. *PloS One*. 2014;9:e90390.
17. Mowat FM, Petersen-Jones SM, Williamson H, et al. Topographical characterization of cone photoreceptors and the area centralis of the canine retina. *Mol Vis*. 2008;14:2518–2527.
18. The American Kennel Club. *How to calculate dog years to human years*. Available at: https://www.akc.org/expert-advice/health/how-to-calculate-dog-years-to-human-years/. Accessed March 21, 2021.
19. Wang T, Ma J, Hogan AN, et al. Quantitative translation of dog-to-human aging by conserved remodeling of the DNA methylome. *Cell Syst*. 2020;11:176–185.e6.
20. Sparrow JR, Duncker T, Schuerch K, Paavo M, de Carvalho JRL Lessons learned from quantitative fundus autofluorescence. *Prog Retin Eye Res*. 2020;74:100774.
21. Lesiuk TP, Braekevelt CR. Fine structure of the canine tapetum lucidum. *J Anat*. 1983;136:157–164.
22. Usher CH. A note on the dog's tapetum in early life. *Br J Ophthalmol*. 1924;8:357–361.
23. Yamaue Y, Hosaka YZ, Uehara M. Macroscopic and histological variations in the cellular tapetum in dogs. *J Vet Med Sci*. 2014;76:1099–1103.
24. Greenstein VC, Schuman AD, Lee W, et al. Near-infrared autofluorescence: its relationship to short-wavelength autofluorescence and optical coherence tomography in recessive Stargardt disease. *Invest Ophthalmol Vis Sci*. 2015;56:3226–3234.
25. Song H, Rossi EA, Latchney L, et al. Cone and rod loss in Stargardt disease revealed by adaptive optics scanning light ophthalmoscopy. *JAMA Ophthalmol*. 2015;133:1198–1203.
26. Schroeder M, Kjellstrom U. Full-field ERG as a predictor of the natural course of ABCA4-associated retinal degenerations. *Mol Vis*. 2018;24:1–16.
27. Strauss RW, Munoz B, Ho A, et al. Progression of Stargardt disease as determined by fundus autofluorescence in the retrospective Progression of Stargardt Disease Study (ProgStar Report No. 9). *JAMA Ophthalmol*. 2017;135:1232–1241.
28. Taubitz T, Tschulakow AV, Tikhonovich M, et al. Ultrastructural alterations in the retinal pigment epithelium and photoreceptors of a Stargardt patient and three Stargardt mouse models: indication for the central role of RPE melanin in oxidative stress. *Peer J*. 2018;6:e5215.
29. Sparrow JR, Yoon KD, Wu Y, Yamamoto K. Interpretations of fundus autofluorescence from studies of the bisretinoids of the retina. *Invest Ophthalmol Vis Sci*. 2010;51:4351–4357.
30. Birch DG, Peters AY, Locke KL, Spencer R, Megarity CF, Travis GH. Visual function in patients with cone-rod dystrophy (CRD) associated with mutations in the ABCA4(ABCR) gene. *Exp Eye Res*. 2001;73:877–886.
31. Fujinami K, Lois N, Davidson AE, et al. A longitudinal study of Stargardt disease: clinical and electrophysiologic assessment, progression, and genotype correlations. *Am J Ophthalmol*. 2013;155:1075–1088.e1013.

32. Klevering BJ, van Driel M, van de Pol DJ, Pinckers AJ, Cremers FP, Hoyng CB. Phenotypic variations in a family with retinal dystrophy as result of different mutations in the ABCR gene. *Br J Ophthalmol*. 1999;83:914–918.
33. Del Pozo-Valero M, Riveiro-Alvarez R, Blanco-Kelly F, et al. Genotype-phenotype correlations in a Spanish cohort of 506 families with biallelic ABCA4 pathogenic variants. *Am J Ophthalmol*. 2020;219:195–204.
34. Kitiratschky VB, Grau T, Bernd A, et al. ABCA4 gene analysis in patients with autosomal recessive cone and cone rod dystrophies. *Eur J Hum Genet*. 2008;16:812–819.
35. Klevering BJ, Blankenagel A, Maugeri A, Cremers FP, Hoyng CB, Rohrschneider K. Phenotypic spectrum of autosomal recessive cone-rod dystrophies caused by mutations in the ABCA4 (ABCR) gene. *Invest Ophthalmol Vis Sci*. 2002;43:1980–1985.
36. Lee W, Paavo M, Zernant J, et al. Modification of the PROM1 disease phenotype by a mutation in ABCA4. *Ophthalmic Genet*. 2019;40:369–375.
37. Fritsche LG, Fleckenstein M, Fiebig BS, et al. A subgroup of age-related macular degeneration is associated with mono-allelic sequence variants in the ABCA4 gene. *Invest Ophthalmol Vis Sci*. 2012;53:2112–2118.
38. Sears AE, Bernstein PS, Cideciyan AV, et al. Towards treatment of Stargardt disease: workshop organized and sponsored by the Foundation Fighting Blindness. *Transl Vis Sci Technol*. 2017;6:6.